

Study of Ion Transport in Lithium Perchlorate-Succinonitrile Plastic Crystalline Electrolyte via Ionic Conductivity and in Situ Cryo-Crystallography

Supti Das, Siriyara J. Prathapa, Pramod V. Menezes, Tayur N. Guru Row, and Aninda J. Bhattacharyya*

Solid State and Structural Chemistry Unit, Indian Institute of Science, Bangalore 560012, India

Received: October 25, 2008; Revised Manuscript Received: February 6, 2009

Ion transport mechanism in lithium perchlorate (LiClO_4)-succinonitrile (SN), a prototype of plastic crystalline soft matter electrolyte is discussed in the context of solvent configurational isomerism and ion solvation. Contributions of both solvent configurational isomerism and ion solvation are reflected in the activation energy for ion conduction in 0–1 M LiClO_4 –SN samples. Activation energy due to solvent configurational changes, that is, trans–gauche isomerism is observed to be a function of salt content and decreases in presence of salt (except at high salt concentrations, e.g. 1 M LiClO_4 –SN). The remnant contribution to activation energy is attributed to ion-association. The X-ray diffraction of single crystals obtained using in situ cryo-crystallography confirms directly the observations of the ionic conductivity measurements. Fourier transform infrared spectroscopy and NMR line width measurements provide additional support to our proposition of ion transport in the prototype plastic crystalline electrolyte.

1. Introduction

Soft matter ionic conductors^{1–13} generally are comprised of an ionic salt solvated in a soft matrix such as apolymer^{1–3} or plastic crystal.^{6–11} High ambient temperature ionic conductivity (10^{-3} – $10^{-2} \Omega^{-1}\text{cm}^{-1}$), compliant mechanical property, wide electrochemical voltage window, and higher safety have resulted in preference of these materials over the conventional crystalline solid ionic conductors for the development of all solid-state electrochemical devices such as rechargeable lithium batteries.² Macroscopic material properties of soft matter electrolytes have been observed to be heavily influenced by various intrinsic physicochemical features of the soft matter solvent. Material property optimization procedures must necessarily account for the intrinsic complexities such as solvent molecular dynamics, ion solvation for tailoring materials for applications. Polymer electrolytes^{1–4} are the most widely studied soft matter electrolytic system where ion transport (above polymer glass transition temperature, T_g) is aided by segmental motion of polymer chains. Segmental motion of polymer chains is further correlated to the microstructure with larger mobilities in amorphous regions compared to crystalline counterparts. Research efforts in improving ambient temperature ionic conductivity ($\leq 10^{-6} \Omega^{-1}\text{cm}^{-1}$) of polymer electrolytes have generally aimed at developing polymeric systems with low degree of crystallinity. In this context, two of the most widely employed approaches have been (a) heterogeneous doping¹⁴ of polymer electrolytes with surface functionalized oxide materials^{15,16} and (b) incorporation of nonaqueous molecular liquid solvents to form gel electrolytes.¹⁷ However, both approaches fail to optimize materials' properties requisite for electrochemical applications. Recently, against conventional thought appreciable ambient temperature ionic conductivity has also been demonstrated in short chain polydisperse crystalline polymer electrolytes.³ However, the potential of the crystalline polymer electrolytes cannot be judged presently as the ambient temperature ionic

conductivity is still not very promising. In light of several unsuccessful attempts at optimizing polymer electrolyte ionic conductivity to values typical of conventional nonaqueous liquid electrolytes ($\sim 10^{-2} \Omega^{-1}\text{cm}^{-1}$), recent years have seen an upsurge in research activity on soft matter electrolytes based on plastic crystalline^{6–11} and ionic liquids.¹²

Effect of plasticity which is due to presence of high concentration of defects such as vacancies, dislocations has been observed in a wide variety of materials ranging from metals¹⁸ to organic compounds such as cyclohexane.¹⁹ In organic materials, plasticity originates from orientational disorder of a molecular group.^{19,20} In the realm of ionics, plasticity arising out of rotational disorder was first reported with regard to inorganic materials such as Li_2SO_4 ,²¹ and NH_4Cl .²² At $T \geq 575^\circ\text{C}$, Li_2SO_4 transforms from the normal crystalline to plastic crystalline phase via the activation of SO_4^{2-} rotatory motions. Fast ion transport of the Li^+ ion takes place via the revolving door mechanism of the SO_4^{2-} ion.²¹ As the transformation to high conducting plastic phase takes place at temperatures higher than ambient, inorganic materials such as Li_2SO_4 are not suitable for electrochemical applications for operation at ambient conditions. Contrary to inorganic materials, several organic exhibit plasticity at much lower temperatures (less than 100°C). Quaternary ammonium,²³ pyrrolidinium (Py),⁶ or imidazolium (Im)⁶-based compounds are some of the well-known examples and have been demonstrated to be promising matrices for solvation of various lithium salts. Succinonitrile^{7–11} ($\text{N}\equiv\text{C}-\text{CH}_2-\text{CH}_2-\text{C}\equiv\text{N}$; SN; dielectric constant, $\epsilon = 55$) is a highly polar solid organic molecular plastic material. Unlike the undoped Py/Im-based plastic electrolytes, undoped SN is nonconducting at ambient temperature. Because of its nonion-icity and high polarity, SN forms a promising solvent for generation of solid ionic conductors with high ambient temperature ionic conductivity. The salt-SN electrolytic systems are conducting only in the plastic solid phase of SN ($\sim 30^\circ\text{--}60^\circ\text{C}$, body-centered cubic) due to presence of orientational disorder. (In the molten phase, ion conduction mechanism is similar to that of a molecular solvent such as acetonitrile.) The

* To whom correspondence should be addressed. E-mail: aninda_jb@sscu.iisc.ernet.in. Tel: +91 80 22932616. Fax: +91 80 23601310.

orientational disorder originates from trans-gauche isomerism involving rotation of molecules about the central C–C bond.^{7,8,20} It has been proposed that trans isomer acts as an impurity resulting in enhancement of lattice defects and lowering of activation energy for ionic conduction. At $T < T_{np}$, SN exists only in the “gauche” conformation and all rotatory motions are frozen (monoclinic). The ionic conductivity of LiX-SN in the normal crystalline phase is expected to be significantly lower than that in the plastic phase. While published reports^{7–11} have so far concentrated on the applicability of SN-plastic electrolytes for electrochemical applications, there are no reports focused on correlation of ion transport with structure. We present here a detailed study of ion transport in the context of solvent configurational isomerism and ion solvation based on ionic conductivity (ac-impedance spectroscopy) and single crystal X-ray studies (in situ cryo-crystallography) in LiClO₄-SN, a prototype plastic crystalline electrolyte. Observations from ionic conductivity and X-ray diffraction studies are further supplemented by differential scanning calorimetry, Fourier transform infrared spectroscopy, and NMR.

2. Experimental Materials and Methods

Electrolyte Preparation and Ionic Conductivity Measurement Using ac-Impedance Spectroscopy. Prior to electrolyte preparation, lithium perchlorate (LiClO₄, lithium battery grade, Chemetall GmbH) was heated at 110 °C under vacuum for removal of physisorbed water. Succinonitrile (SN, Aldrich) was sublimated twice to remove impurities. Requisite amount of LiClO₄ ($x = 0.005$ –1 M) was added to molten SN and stirred at 60 °C under dry N₂ atmosphere until a homogeneous mixture was obtained. The solidified melt was stored in glass vials under vacuum at 25 °C until further use. Homogeneous transparent samples were obtained for all concentrations of LiClO₄. For conductivity measurements, the molten LiClO₄-SN sample was poured directly into an airtight home-built conductivity cell. The conductivity cell was assembled inside an argon filled glovebox (MBraun MB 20G LMF; water: < 0.1 ppm) and was inserted into a glass jacket having provisions for measuring under dynamic vacuum (pressure = 1 mbar). The cell constant for all samples was approximately 0.05 cm⁻¹. For ionic conductivity measurement versus temperature (range: –45–70 °C) the cell and glass jacket combination was immersed in a thermostat (FP50MC Julabo) containing water/ethylene glycol (1:1 v/v) mixture or ethanol. Ionic conductivity was estimated from ac-impedance spectroscopy (Novocontrol Alpha-A) over the frequency range 1–3 × 10⁶ Hz (signal amplitude = 0.05 V).

In Situ X-ray Cryo-Crystallography. Samples for differential scanning calorimetry (Mettler Toledo DSC 823^o) measurements were loaded (under argon) in hermetically sealed aluminum crucibles and cooled down to 80 °C. Data was collected from –80–70 °C with a heating rate of 5 °C/min. Single crystals were grown via the method of *in situ* cryo-crystallography.^{24–27} Sealed Lindemann glass capillary of length ~2 cm and diameter = 0.3 mm filled with SN or LiClO₄-SN was mounted on a Bruker AXS X-ray diffractometer equipped with a SMART APEX CCD area detector. The rate of cooling was ascertained based on the differential scanning calorimetry (DSC). Cooling at 20 K h⁻¹ (OXFORD Nitrogen cryosystem) resulted in complete solidification of the liquid in the capillary at 215 K (–58 °C). It is to be noted that solidification at rates different from 20 K h⁻¹ such as 30–45 K h⁻¹ resulted in the formation of glassy/polycrystalline solid material. To obtain a single crystal inside the capillary, the solid was annealed by shifting the nitrogen stream away from the

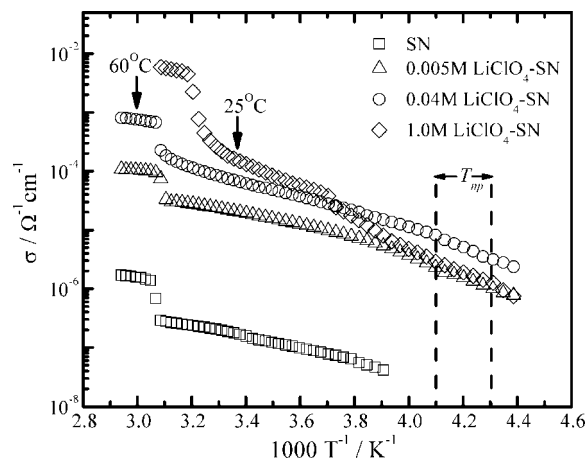


Figure 1. Composite ionic conductivity of 0–1 M LiClO₄-SN versus temperature (range: –45–70 °C). All samples were prepared under nitrogen atmosphere and ionic conductivity was measured every 2 °C under dynamic vacuum (pressure = 1 mbar).

capillary. The solid was allowed to melt partially inside the capillary and then the nitrogen stream was reset at a very slow rate. This procedure was repeated manually until a good single crystal was obtained which can be verified by recording the diffraction pattern. The sample was cooled to 150 K (–123 °C) to minimize thermal vibrations and allowed 1 h stabilization. Subsequently 180 frames of data were collected with 2θ fixed at –25° with a ω scan width of –1.0°. These frames were analyzed using RLATT to determine the unit cell dimensions. Data were collected on three sets of 606 frames with $2\theta = -25^\circ$ and with φ values of 0, 90, and 180°, respectively. The crystal structure was solved and refined using the package SHELX97.^{28–31}

Fourier Transform Infrared Spectroscopy and NMR. Microstructural investigations were also done using Fourier transform infrared (FTIR, Perkin-Elmer FTIR Spectrometer Spectrum 1000) spectroscopy and solid-state NMR. For FTIR, requisite amount of molten electrolyte was added to spectroscopic grade KBr and pressed to form pellets with diameter and thickness equal to 13 mm and 1 mm, respectively. The ¹H NMR and ⁷Li line width ($\Delta\nu$) as a function of temperature were performed on Bruker DSX 300 MHz NMR spectrometer operating at a Larmor frequency of 300.14 and 116.6 MHz, respectively. The line width measurements were carried out giving a $\pi/2$ pulse of 4 μ s sequence. At all temperatures, the probe head was equilibrated for at least 20 min before data collection. The full width at half-maximum ($\Delta\nu$ – x , $x = ^1\text{H}$, ⁷Li) were obtained via fitting of the peaks using Gaussian distribution function.

3. Results and Discussion

Ionic Conductivity from ac-Impedance Spectroscopy. Figure 1 shows the ionic conductivity (σ) as a function of temperature –45–70 °C for 0–1 M LiClO₄-SN. For SN, accurate determination of ionic conductivity was not possible in the temperature regime corresponding to the normal crystalline phase. Because of an increase in sample resistance, the impedance spectra were noisy and it was not possible to fit impedance data (ZView V2.6b, Scribner Associates). For all samples, the impedance spectrum in the molten phase is comprised of a spike that corresponds to the electrode–electrolyte interface.³² The intersection of the spike with the real impedance axis was taken as the sample resistance. In the plastic phase, from temperatures in the vicinity of T_m to approximately room

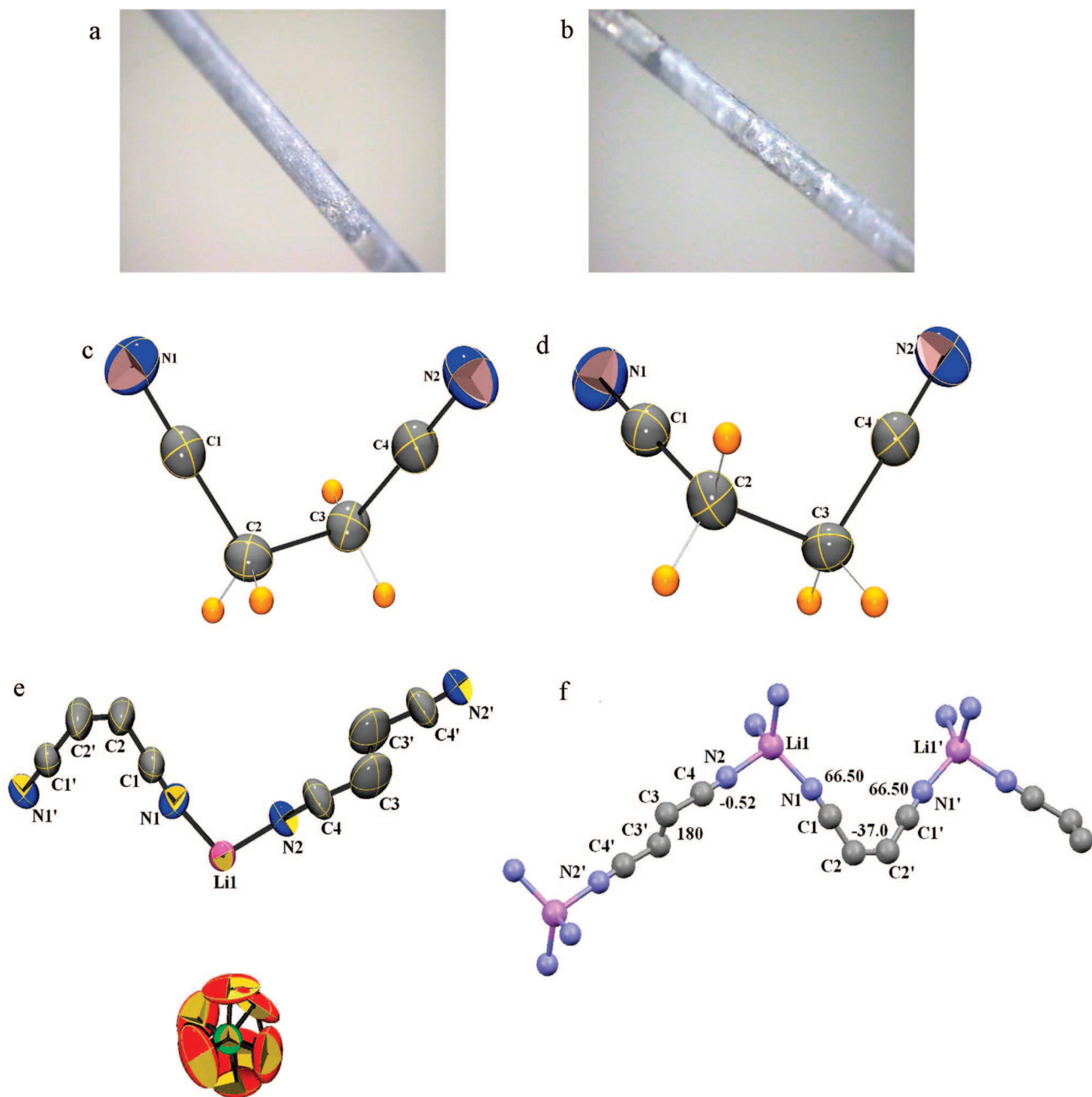


Figure 2. Photograph of single crystals of (a) 0.005 M LiClO₄-SN and (b) 0.3 M LiClO₄-SN. ORTEP diagrams for (c) SN, (d) 0.04 M LiClO₄-SN, (e) 1 M LiClO₄-SN including the disordered perchlorate unit and (f) the torsion angles for the trans and gauche conformers for the 1 M LiClO₄-SN sample.

temperature (≈ 25 °C) impedance spectra comprises of a low frequency spike (due to electrode-electrolyte interface) and a high frequency arc. With further decrease in temperature for $T \leq T_{np}$, the high frequency arc developed in to a semicircle. Intersection of spike with the arc or semicircle was taken as the sample resistance. Analysis of the impedance spectra showed that the semicircle truly reflected bulk properties ($\epsilon = 50$ from impedance spectra³²). Further, a certain degree of hysteresis was observed in plastic crystalline ($\approx 30\%$) and normal crystalline phase ($\approx 35\%$) for all samples with conductivity being higher for first cooling cycle compared to first heating cycle. As no significant hysteresis was observed between conductivity data of first cooling and subsequent heating/cooling cycles, we discuss here only ionic conductivity data for the first cooling cycle. Ionic conductivity in the molten temperature did not exhibit any hysteresis. Samples prepared under nitrogen atmo-

sphere and ionic conductivity measured under dynamic vacuum were highly reproducible. Measurement of samples prepared and measured under different experimental conditions (cf. Supporting Information) were also reproducible and very similar to that of samples prepared under nitrogen atmosphere and ionic conductivity measured under dynamic vacuum. Ionic conductivity versus temperature data in general was approximated as a three step activation process corresponding to molten, plastic crystalline, and normal crystalline phases. The activation energy (E_a) pertaining to respective phases was obtained by fitting conductivity data with Arrhenius equation. Although pure SN is expected to be ionically nonconducting, measurable conductivities in the range 4.0×10^{-8} to $2 \times 10^{-6} \Omega^{-1} \text{cm}^{-1}$ (at 25 °C, $\sigma = 3.1 \times 10^{-7} \Omega^{-1} \text{cm}^{-1}$) were recorded in the plastic phase -30 – 58 °C. E_a in plastic phase was approximately 0.22 eV, which is very similar to activation energy values equal to

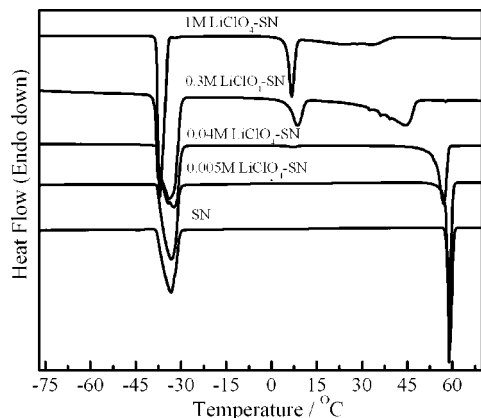


Figure 3. Differential scanning calorimetry (DSC) for 0–1 M LiClO_4 –SN.

0.20 eV corresponding to trans–gauche dynamics obtained from optical experiments.³³ In the molten regime, E_a was estimated to be 0.19 eV. It has been proposed that existence of impurities in plastic materials could give rise to lowering of activation energies and higher conductivities.^{19,20} We attribute the observed conductivity of SN to be due to some remnant impurity (such as ionic salts) which could not be removed even after a two step sublimation process. Similarity in E_a values for SN with that of conformational isomerism strongly suggests that ion transport at very dilute dopant concentrations is rate limited by the solvent trans–gauche isomerism.

Addition of LiClO_4 to SN resulted in a drastic increase in ionic conductivity compared to undoped SN. Ionic conductivity enhancement was more than 2 orders in the plastic phase and 2–4 orders in the melting phase. The temperature variation of conductivity is marked by an almost linear increase in the plastic phase followed by a jump (few times to 1.5 orders) in conductivity across the melting temperature ($T_m \sim 40^\circ\text{C}$). In the plastic phase, the E_a values for 0.005–1 M LiClO_4 –SN samples were in the range 0.22–0.49 eV (for SN $E_a = 0.20$ eV). In the molten phase, the E_a values for the doped SN samples decreased and were in the range 0.1–0.25 eV. In the solid plastic phase, both trans–gauche isomerism and ion association (electrostatic interaction) contribute to activation energy, where molten phase is solely governed by ion association similar to that of conventional molecular solvents ($E_{a\text{-molten}} \approx E_{\text{association}}$). The presence of salt influences the SN microstructure in several ways. Local solvation of ions (in addition to temperature³⁴) leads to a decrease in the trans–gauche energy barrier and hence an increase in disorder. The trans concentration is expected to be higher with simultaneous increase in defect concentration.³⁵ This accounts for the reduction in E_a values for conformational dynamics (i.e., trans–gauche isomerism) from 0.2 eV in undoped SN to approximately 0.15 eV for 0.005M/0.04 M LiClO_4 –SN samples. Further, presence of salt in substantial amount (such as 1 M) may also lead to enhancement of overall crystallinity¹⁰ in the sample (DSC: Figure 3) and subsequent reduction in the conformational dynamics. This is probably the reason why E_a values for conformational dynamics in the case of 1 M LiClO_4 –SN samples are similar to that for undoped SN. In order to confirm the role of ion association in LiClO_4 –SN, ionic conductivity of 0.04 and 1 M LiClO_4 in anhydrous acetonitrile (ACN) were measured in the temperature range -37 to 55°C . The activation energy obtained by Arrhenius fitting of conductivity data were 0.1 eV for 0.04 M LiClO_4 –ACN and 0.25 eV for 1 M LiClO_4 –ACN. The E_a values for LiClO_4 –ACN samples are nearly equal to the

decrement in E_a values in going from the solid plastic to molten phase for the respective LiClO_4 –SN concentration. As no conformational isomerism exists in acetonitrile, the contribution to activation energy for LiClO_4 –ACN is entirely due to ion association. On the basis of the activation energy values for ion conduction we propose that in addition to trans–gauche isomerism solvation in the form of ion association also plays a significant role in determining ion transport. Ion association is substantial at higher salt concentration and this is evident from lower ionic conductivity of 1 M LiClO_4 –SN compared to 0.04 M LiClO_4 –SN for $T < -5^\circ\text{C}$.

In Situ X-ray Cryo-Crystallography. Observations from ionic conductivity are directly confirmed by X-ray diffraction of single crystals grown via in situ cryo-crystallography. In situ cryo crystallization has been previously successfully employed for a wide variety of organic material^{24–27} including imidazolium based ionic liquids. Good quality single crystals (Figure 2a,b) were obtained via an optimized cooling and annealing protocol. SN crystallizes in a monoclinic system at 150 K (-123°C , Figure 2c), space group $P2_1/c$, with unit cell parameters $a = 5.857(2)\text{Å}$, $b = 8.586(3)\text{Å}$, $c = 9.114(3)\text{Å}$, $\beta = 100.646(2)^\circ$, and $V = 450.4(3)\text{Å}^3$ with $Z = 4$. The packing in the crystal lattice is essentially through van der Waals interactions. The torsion angle C1–C2–C3–C4 in Figure 2c is $61.54(18)^\circ$ confirming that SN is in a gauche conformation as reported in earlier literature.^{7,8,19,20} At 150 K, 0.04 M LiClO_4 –SN (Figure 2d) also crystallizes in a monoclinic crystal system in space group $P2_1/c$ (Figure 2d) with similar cell parameters $a = 5.8519(9)\text{Å}$, $b = 8.5804(14)\text{Å}$, $c = 9.1119(15)\text{Å}$, $\beta = 100.574(2)^\circ$, $V = 449.75(13)\text{Å}^3$ with $Z = 4$. The structure remains unaltered at this composition with the torsion angle C1–C2–C3–C4 equal to $61.55(12)^\circ$. According to DSC, as these temperatures (i.e., -123°C) are below T_{mp} , the 0.04 M LiClO_4 –SN sample is expected to be in the normal crystal phase and the X-ray diffraction results confirm this observation. Influence of ion association on the crystallographic structure could not be ascertained due to low salt content. The 1 M LiClO_4 –SN (Figure 2e) crystallizes in an orthorhombic system, space group $Pban$, with cell parameters $a = 10.961(5)\text{Å}$, $b = 21.376(5)\text{Å}$, $c = 5.494(5)\text{Å}$, $V = 1287.3(13)\text{Å}^3$ with $Z = 4$ (data collected at 250K or -23°C). It is noteworthy that attempts to obtain data sets at 150 K as was done in the previous concentrations yielded poor quality data. We believe that this may be due to statistical disorder that might have developed in the crystal in its plastic phase. In spite of this, data was collected at warming steps of every 20 K and it was found that the best resolved data could be obtained only at 250K (-23°C). This observation is substantiated after determining the crystal structure. The Li atom is in a tetrahedral coordination with the nitrogen atoms of SN resulting in both gauche and trans conformers in the asymmetric unit. The perchlorate is disordered as can be expected in this type of crystalline materials. The trans–gauche isomerism is evident from the calculation of the torsion angles. The value of the torsion angle Li1–N1–C1–C2 is 66.50° (Figure 2f) confirming the gauche nature whereas the torsion angles $\text{Li1–N2–C4–C3} = -0.52^\circ$ and $\text{C4–C3–C3'–C4'} = 180^\circ$ confirm the trans configuration. The coordination of Li^+ to CN^- with a disordered ClO_4^- ion in the vicinity suggests the existence of ion-association, being predominant at higher salt concentrations. The single crystal structures obtained for 0–1 M LiClO_4 –SN confirm our proposition that ion transport in LiClO_4 –SN is influenced by both solvent configurational isomerism and ion-association.

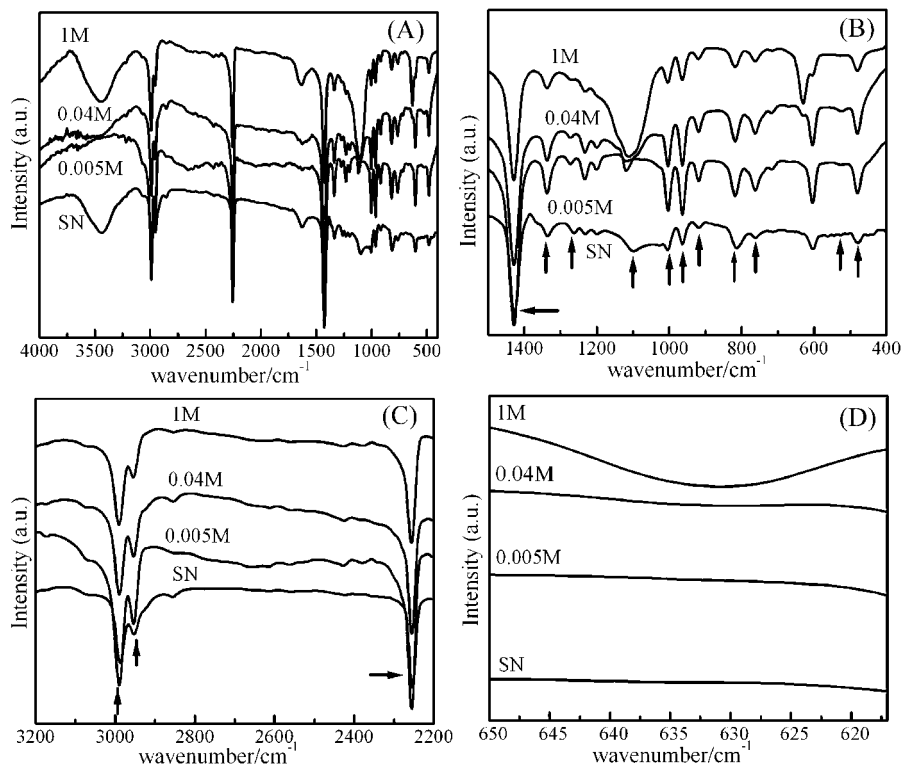


Figure 4. Fourier transform infrared (FTIR) spectra at 25 °C for (0–1)M LiClO₄–SN.

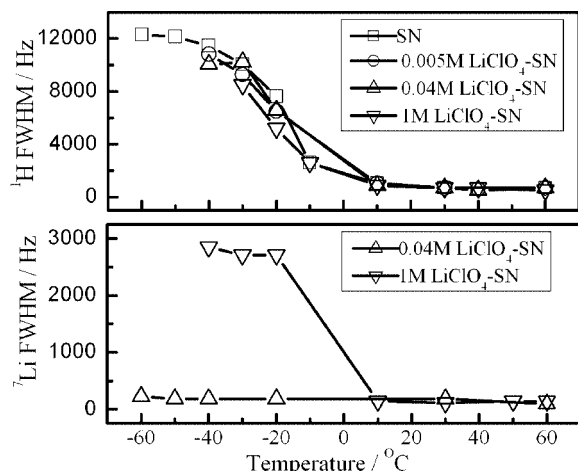


Figure 5. NMR line width for ¹H and ⁷Li versus temperature for 0–1 M LiClO₄–SN.

Differential Scanning Calorimetry. Figure 3 shows the differential scanning calorimetry plots for (0–1) M LiClO₄–SN samples. For pure SN, peaks at –33 and 59 °C^{7–11} correspond respectively to normal to plastic crystal, T_{np} , and melting, T_m transitions. For 0.005 M LiClO₄–SN, T_{np} was very similar to SN. However, significant changes in T_{np} was observed for salt concentrations higher than 0.005 M. The observance of multiple peaks or shift in T_{np} for salt concentrations higher than 0.005 M LiClO₄–SN is correlated to SN trans–gauche isomerism. As remarked earlier, presence of impurity in general, reduces the trans–gauche energy barrier compared to that in pure SN.^{19,20} This results in a faster transition rate to the high defect density trans state and also existence of SN in trans conformation at temperatures even lower than T_{np} of undoped SN. The fraction of SN molecules whose normal to plastic crystal transition have been affected depend on salt concentration being higher for higher salt concentrations. This accounts for

the observation of multiple peaks in the range –32 to –37.5 °C for 0.04 M LiClO₄–SN and 0.3 M LiClO₄–SN samples. The peak observed at lower temperature (such as at –32 °C) is attributed to SN molecules unaffected by salt addition. In a heavily doped sample such as 1 M LiClO₄–SN, a high probability exists that trans–gauche isomerism of majority of SN molecules are affected due to salt addition resulting in a clear shift in T_{np} to –37 °C. The observance of two or more solid phase transitions in doped SN materials has not been reported earlier^{7,8,10} probably because published results were with salt concentrations of nearly equal to 1 M.

Noticeable changes in the melting transition are also observed with regard to both dilute and concentrated samples of LiClO₄–SN. For the 0.005 and 0.04 M samples T_m shifted to lower temperatures by 1 and 3 °C, respectively. For 0.3 and 1 M samples in addition to shifts in T_m , peak broadening and additional peaks were also observed. The additional peaks are attributed to the formation of LiClO₄–SN complexes, which is supported by single crystal X-ray and FTIR studies (Figure 4). The LiClO₄–SN complexes are also probably responsible for inducing local ordering thus increasing the crystallinity of the sample.¹⁰

Fourier Transform Infrared Spectroscopy. Evidence of existence of different isomeric conformers and ion-association can be inferred from Fourier transform infrared (FTIR) spectroscopy.³⁵ This has been recently successfully demonstrated in the context of plastic-polymer composite electrolytes.¹⁰ Figure 4A–D shows the room temperature FTIR spectra for various samples. Influence on trans–gauche isomerism due to variation in additive concentration and temperature³⁵ can be studied via changes occurring at the following signature bands (Figure 4A–C): 478 cm^{–1} (C–C–C bending, gauche), 530 cm^{–1} (C–C–C bending, trans), 601 cm^{–1} (C–C–C bending, gauche), 760 cm^{–1} (CH₂ rocking, trans), 819 cm^{–1} (CH₂ bending, gauche), 917 cm^{–1} (C–CN stretch, trans), 963 cm^{–1} (C–CN, gauche), 1004 cm^{–1} (CH₂, gauche), 1098 cm^{–1} (CH₂, gauche),

1270 cm^{-1} (CH_2 wagging, trans), 1335 cm^{-1} (CH_2 bending, gauche), 1424 cm^{-1} (CH_2 bending, gauche and trans), 2254 cm^{-1} ($\text{C}\equiv\text{N}$ stretching, gauche and trans), 2953 cm^{-1} ($\text{C}-\text{H}$, gauche and trans), and 2990 cm^{-1} ($\text{C}-\text{H}$ stretching, gauche and trans). For doped SN samples, the above bands became sharper and more intense compared to undoped SN. Observed changes in band intensity and contour are attributed to several factors. Increase in intensity of bands for the doped SN samples compared to undoped SN is attributed to increased trans–gauche isomerism. Higher intensity of 530, 760, and 917 cm^{-1} bands in LiClO_4 –SN compared to SN suggest increase in trans concentration. On the other hand, sharpening of band contour is due to enhancement in overall crystallinity of LiClO_4 –SN samples. Enhancement in crystallinity is due to the formation of several LiClO_4 –SN complexes (cf. DSC, Figure 3). The complexes are formed due to the interaction between Li^+ and CN^- and sharpening of bands at 917, 963, and 2254 cm^{-1} (Figure 4B,C) in 0.005–1 M LiClO_4 –SN serve as a strong evidence for the existence for such an interaction. It is to be noted that conformer bands for 1 M LiClO_4 –SN were less intense in comparison to 0.005M/0.04 M LiClO_4 –SN samples. This is due to direct Li^+ coordination to CN^- . Signature of ion-association in the way of a broadband between 625–637 cm^{-1} (Figure 4D) is observed predominantly in case of 1 M LiClO_4 –SN sample. The band attributed to Li^+ – ClO_4^- contact ion-pair usually appears at 637 cm^{-1} whereas the band at 627 cm^{-1} is due to free ClO_4^- anion.³⁶ In our study, both bands could not be separately resolved; however the 1 M LiClO_4 –SN sample showed a much more intense band compared to the dilute salt samples. The formation of solvent shared ion pairs is directly supported by single crystal X-ray studies.

Line Width versus Temperature from NMR Studies.

Figure 5 shows temperature variation of full width at half-maximum ($\Delta\nu$ –x; x: ^1H , ^7Li). For all samples $\Delta\nu$ – ^1H decreases by an order of magnitude in the temperature range -40°C ($\sim T_{\text{np}}$) to 10°C . Decrease in $\Delta\nu$ – ^1H is attributed to the transition of SN from a nonrotator (predominantly gauche) normal crystalline to a rotator (mixed trans and gauche; liquidlike) plastic crystalline phase. No further narrowing was observed for $T > 10^\circ\text{C}$ through the melting temperature (T_{m}). This is a direct consequence of the high degree of disorder already present in the solid plastic phase. It is interesting to observe the variation in $\Delta\nu$ – ^7Li versus temperature for 0.04 and 1 M samples. (For 0.005 M sample, accurate determination of $\Delta\nu$ – ^7Li was not possible due to low lithium content.) For 1 M LiClO_4 –SN, $\Delta\nu$ – ^7Li changes by one order in magnitude in the vicinity of T_{np} similar to that $\Delta\nu$ – ^1H . The changes in $\Delta\nu$ – ^7Li for 0.04 M LiClO_4 –SN are much less (≈ 1.5 times). For 0.04 M LiClO_4 –SN sample majority of Li^+ ions are free and ion-association will have no influence on line width. Lithium has a liquidlike environment for both $T > T_{\text{np}}$ and $T < T_{\text{np}}$. However, for 1 M LiClO_4 –SN, $\Delta\nu$ variation with temperature is influenced by both trans–gauche isomerism and ion-association. For $T > T_{\text{np}}$, variation in $\Delta\nu$ – ^7Li versus temperature for both 1 M LiClO_4 –SN and 0.04 M LiClO_4 –SN are similar due to initiation of rotational disorder. However, for $T < T_{\text{np}}$ $\Delta\nu$ – ^7Li for 1 M LiClO_4 –SN is considerably broader compared to 0.04 M LiClO_4 –SN sample. NMR accounts for all Li^+ nuclei present in the sample including the fraction in the solvent shared ion-pairs. As the ion pairing is substantial for 1 M LiClO_4 –SN, Li^+ dynamics is substantially reduced for $T < T_{\text{np}}$ leading to broadening of the ^7Li line.

4. Conclusions

We have vividly demonstrated here the influence of solvent configurational isomerism and ion solvation on ion transport in LiClO_4 –SN, a prototype plastic crystalline electrolyte. Structural investigations, especially X-ray diffraction of single crystals, directly support the proposition for ion transport based on observations from ionic conductivity studies. The successful outcome of using in situ cryo-crystallography for growing good quality single crystals of plastic crystalline materials promises application of the same to study ion conduction mechanism of other important contemporary soft matter ionic conductors such as ionic liquid electrolytes. Configurational isomerism depends both on temperature as well as on salt concentration. Higher temperature and salt content results in higher degree of disorder and faster conformational dynamics. However, higher salt content results in substantial ion association that is detrimental for achieving high ionic conductivity. We believe that fundamental studies like the present one would help in identifying the parameters whose optimization is crucial for designing electrolytic materials for electrochemical applications.^{10,11}

Acknowledgment. The authors acknowledge I.S. Jarali for DSC and FTIR, C. Panitz, Chemetall GmbH., Germany for lithium battery grade LiClO_4 . We thank the Department of Science and Technology, India, for use of the CCD facility setup under the IRHPA-DST program at IISc. S.D. thanks CSIR for Junior Research Fellowships and A.J.B. thanks Department of Science and Technology, India for research funding under SR/S1/PC-07/2007. P.V.M. thanks STC ISRO-IISc for Project Assistantship. As the work was initiated at Max Planck Institute of Solid State Research, Stuttgart, Germany, the authors acknowledge Professor J. Maier and Dr. S. Hore for useful discussions and E. Schmitt and W. König, respectively, for some preliminary DSC and FTIR measurements.

Supporting Information Available: Ionic conductivity of various 1 M LiClO_4 –SN samples as a function of temperature (Figure S1). This material is available free of charge via the Internet at <http://pubs.acs.org>.

References and Notes

- (1) (a) Fenton, D. E.; Parker, J. M.; Wright, P. V. *Polymer* **1973**, *14*, 589. (b) Shriver, D. F.; Bruce, P. G. *Solid State Electrochemistry*; Bruce, P. G. Ed.; Cambridge University Press: Cambridge, 1995; pp 95–118. (c) Gray, F. M.; Armand, M. *Handbook of battery materials*; Besenhard, J. O. Ed.; Wiley-VCH: Weinheim, 1999; pp 499–523.
- (2) Bruce, P. G.; Scrosati, B.; Tarascon, J. M. *Angew. Chem., Int. Ed.* **2008**, *47*, 2930–2946.
- (3) Christie, A. M.; Lilley, S. J.; Staunton, E.; Andreev, U. G.; Bruce, P. G. *Nature (London)* **2005**, *433*, 50–53.
- (4) Zhang, C.; Andreev, Y. G.; Bruce, P. G. *Angew. Chem., Int. Ed.* **2007**, *46*, 2848–2850.
- (5) Bhattacharyya, A. J.; Maier, J. *Adv. Mater.* **2004**, *16*, 811–814.
- (6) Macfarlane, D. R.; Huang, J.; Forsyth, M. *Adv. Mater.* **2001**, *13*, 957–966.
- (7) Long, S.; MacFarlane, D. R.; Forsyth, M. *Solid State Ionics* **2003**, *161*, 105–112.
- (8) Alarco, P. J.; Abu-Lebdeh, Y.; Abouimrane, A.; Armand, M. *Nat. Mater.* **2004**, *3*, 476–481.
- (9) Fan, L.-Z.; Hu, Y.-S.; Bhattacharyya, A. J.; Maier, J. *Adv. Func. Mater.* **2007**, *17*, 2800–2807.
- (10) Patel, M.; Chandrappa, K. G.; Bhattacharyya, A. J. *Electrochim. Acta* **2008**, *54*, 209–215.
- (11) Patel, M.; Bhattacharyya, A. J. *Electrochem. Comm.* **2008**, *10*, 1912–1915.
- (12) Shin, J. H.; Henderson, W. A.; Passerini, S. *Electrochem. Comm.* **2003**, *5*, 1016–1020.
- (13) Xu, K. *Chem. Rev.* **2004**, *104*, 4303–4417.
- (14) Maier, J. *Prog. Solid State Chem.* **1995**, *23*, 171–263.

- (15) Croce, F.; Appetecchi, G. B.; Persi, L.; Scrosati, B. *Nature (London)* **1998**, 394, 456–458.
- (16) Croce, F.; Settini, L.; Scrosati, B. *Electrochem. Commun.* **2006**, 8, 364–368.
- (17) Appetecchi, G. B.; Aihara, Y.; Scrosati, B. *Solid State Ionics* **2004**, 170, 63–72.
- (18) *Plasticity of metals and alloys*, ISPMA 6 Proc. 6th Int. Symp. Prague, Czech Republic, September, 1994; Pavel, L. Ed.; Transtec: Switzerland.
- (19) Sherwood, J. N. *The plastically crystalline state*; Sherwood, J. N. Ed.; Wiley: London, 1979.
- (20) Hawthorne, H. M.; Sherwood, J. N. *Trans. Faraday Soc.* **1970**, 66, 1799–1801.
- (21) Aronsson, R.; Jansson, B.; Knape, H. E. G.; Lunden, A.; Nilsson, L.; Sjöblom, C. A.; Torell, L. M. *J. Phys. Colloq.* **1979**, C6, 35–37.
- (22) Tansho, M.; Furukawa, Y.; Nakamura, D.; Ikeda, R. *Ber. Bunsen-Ges. Phys. Chem.* **1992**, 96, 550–553.
- (23) Cooper, E. I.; Angell, C. A. *Solid State Ionics* **1986**, 18 & 19, 570–576.
- (24) Choudhury, A. R.; Winterton, N.; Steiner, A.; Cooper, A. I.; Johnson, K. A. *J. Am. Chem. Soc.* **2005**, 127, 16792–16793.
- (25) Choudhury, A. R.; Winterton, N.; Steiner, A.; Cooper, A. I.; Johnson, K. A. *CrystEngComm* **2006**, 8, 742–745.
- (26) Matsumoto, K.; Hagiwara, R.; Tamada, O. *Solid State Sci.* **2006**, 8, 1103–1107.
- (27) Chopra, D.; Row, T. N. G. *J. Indian. Inst. Sci.* **2007**, 87, 167–211.
- (28) *Bruker SMART (Version 5.628) and SAINT (Version 6.45a)*; Bruker AXS Inc.: Madison, WI, 2004.
- (29) Farrugia, L. J. *J. Appl. Crystallogr.* **1999**, 32, 837–838.
- (30) Sheldrick, G. M. *SHELXL97*; University of Göttingen: Germany, 1997.
- (31) Spek, A. L. *J. Appl. Crystallogr.* **2003**, 36, 7, 13.
- (32) In the plastic phase temperature range the impedance spectra for the bulk was fitted by a resistance, R and constant phase element, CPE (Q_1) in parallel. Capacitance, $C = (R^{1-n} \cdot CPE)^{1/n}$, and $\epsilon_r = (Ck)/\epsilon_0$ where k is the cell constant. The electrode-electrolyte interface (spike) was fitted with another CPE (Q_2) element. The values obtained for Q_2 reflected blocking character of the stainless steel electrode.
- (33) (a) Bischofberger, T.; Courtens, E. *Phys. Rev. Lett.* **1974**, 32, 163–166. (b) Foggi, P.; Righini, R.; Torre, R.; Angeloni, L.; Califoni, S. *J. Chem. Phys.* **1992**, 96, 110–115. (c) Wrðøz, T.; Kubicki, J.; Nasrêcki, R.; Bancewicz, T. *J. Chem. Phys.* **1995**, 103, 9212–9217.
- (34) (a) Janz, G. J.; Fitzgerald, W. E. *J. Chem. Phys.* **1955**, 23, 1973. (b) Fengler, O. I.; Ruoff, A. *Spectrochim. Acta A* **2001**, 57, 105.
- (35) FTIR data recorded at -45°C , that is, $T < T_{np}$ shows presence of trans bands ($\sim 10\%$) for concentrated $\text{LiClO}_4\text{-SN}$ samples.
- (36) Salomon, M.; Xu, M.; Eyring, E. M.; Petrucci, S. *J. Phys. Chem.* **1994**, 98, 8234–8244.

JP809465U